Research Article
Evaluation of Residual Stresses in a Rolled Sheet of AA 6082-T6 Aluminium Alloy

[1]F.V. Díaz, [1]F.N. Rosso, [1]A.C. Walker, [1]C.A. Mammana and [2]A.P.M. Guidobono
[1]Departamento de Ingeniería Electromecánica, Universidad Tecnológica Nacional (FRRa), Acuña 49,
2300 Rafaela, Argentina
[2]División Metrología Dimensional, Instituto Nacional de Tecnología Industrial, Centro Regional Rosario,
Ocampo y Esmeralda, 2000 Rosario, Argentina

Abstract: This study aims to determine and evaluate residual stress components and anisotropy degrees in specimens of a rolled sheet of AA 6082-T6 aluminium alloy. The residual displacements were measured, using an optimised micro-indentation method, with an absolute error down to ±200 nm. A distribution of 8 micro-indents allowed to measure the residual displacements in 5 centroids of several geometric figures associated with that distribution. The results reveal that the normal components are compressive and much higher than the tangential components. The principal directions associated with each centroid were very close to the rolling direction. From the graphical tool called Mohr's circle, it was possible to detect a smooth variation associated with the residual stress state in the rolling direction. Finally, both the residual stress states and anisotropy degrees, evaluated along the rolling direction, would respond to a function which would be similar to the planar rotation function corresponding to the normal and tangential components.

Keywords: Aluminium alloy, anisotropy degree, micro-indent method, Mohr's circle, residual stresses

INTRODUCTION

When a rolled sheet of aluminium alloy for structural use is acquired, the residual stresses previously introduced during the manufacturing process are unknown. These stresses are generated because the material is subjected to inhomogeneous plastic deformation and thermal gradients (Rowlands, 1987; Lu, 1996). It is critical to determine or predict the magnitude, distribution and sign of residual stresses because these can cause early failures. It is noteworthy that these stresses have generated catastrophic failures in many cases (Withers, 2007). Tensile residual stresses are very dangerous since can initiate and propagate fatigue or corrosion cracks (Toribio, 1998; Schwach and Guo, 2006; Coules et al., 2018). On the other hand, compressive residual stresses are usually induced in order to cause opposite effects (Niku-Lari, 1983; Wang et al., 1998; Torres and Voorwald, 2002; Gao et al., 2002). However, in some cases, the failure via compression would be generated due to residual and service stresses add up.

In the last two decades, several methods to determine residual stresses from data generated by micro or nano-indentation have been developed (Suresh and Giannakopoulos, 1998; Lee and Kwon, 2003; Dean et al., 2011). Most of these methods compare the load-displacement curves of stressed and unstressed specimens, from which the normal and tangential stress components can be obtained. Recently, a technique based on the change of coordinates of micro-indents has been developed (Wyatt and Berry, 2006, 2009). This change occurs when the residual stress field relaxes through a thermal distension treatment. More recently, this technique was optimized by incorporating a universal measuring machine, from which it was possible to evaluate, with high precision, normal and tangential components of residual stress generated by low, medium and high-speed milling (Díaz et al., 2010, 2012; Díaz and Mammana, 2012; Díaz et al., 2015). It should be remarked that the present technique of micro-indentation is substantially different from traditional techniques such as the hole drilling method (Rendler and Vigness, 1966) or x-ray diffraction (Noyan and Cohen, 1987) because it does not use specific equipment nor needs highly qualified operators. Also, from this indent method, it is possible to measure residual displacements with an absolute error much lower than that associated with traditional techniques.

The objective of this study is to determine and evaluate normal and tangential components of residual stress in a rolled sheet of AA 6082-T6 aluminium alloy

Corresponding Author: F.V. Díaz, Departamento de Ingeniería Electromecánica-Facultad Regional Rafaela, Universidad Tecnológica Nacional, Acuña 49, 2300 Rafaela, Argentina, Tel.: +54 3492 432710; Fax: +54 3492 422880

for structural use. These components were determined using an optimised micro-indentation approach. It is indispensable to state that, in the literature, there are few studies about residual stresses in the present alloy, which is still relatively new in the market. In this study, from a distribution of 8 micro-indentations, the residual displacements were measured in 5 centroids of different geometric figures associated with that distribution. The measurement error of the residual displacements was less than ±200 nm. The components of the residual stress were computed from those displacements using a plane stress model. Through the graphical tool called Mohr's circle, it was possible to evaluate the components of residual stress in all directions. The results reveal that the normal components are compressive and much higher than the tangential components. The Mohr's circles allowed detecting a smooth gradient associated with the residual stress states in the rolling direction. Furthermore, the principal directions corresponding to each centroid were very close to the rolling direction. Finally, the residual stress states, evaluated along the rolling direction, would respond to a periodic function, which would be similar to the planar rotation function associated with the normal and tangential components.

MATERIALS AND METHODS

This study was wholly performed at the Departamento Ingeniería Electromecánica, Universidad Tecnológica Nacional (Regional Rafaela), in the year 2018.

As aforementioned, the experimental work was carried out from a hot rolled sheet of AA 6082-T6 aluminium alloy of 4 mm thickness. This alloy, which can be considered a relatively new material, is often used to manufacture components of structures for the marine and automotive industries, among others. The different applications of this alloy are based on good physical and mechanical properties and excellent resistance to corrosion. It should be noted that T6 state implies that the aluminium alloy has been thermally treated and then artificially aged. The present work was carried out by using samples whose dimensions were 30×30×4 mm.

The measurement method was performed in two steps. In the first, a distribution of micro-indents was introduced in the surface of the sample using a linear indentation device (Díaz *et al*., 2010) that is coupled to the universal measuring machine (GSIP MU-314). In the second, the coordinates (*x*, *y*, *z*) of each micro-indent were measured, before and after a distension treatment (573 K, 80 min), by using an accuracy microscope that is fixed to the measuring machine (Dotson *et al*., 2003).

The micro-indents were introduced in the vertices of an imaginary square whose side is 21 mm. This square was centred on one face of the sample. Figure 1a

(a)
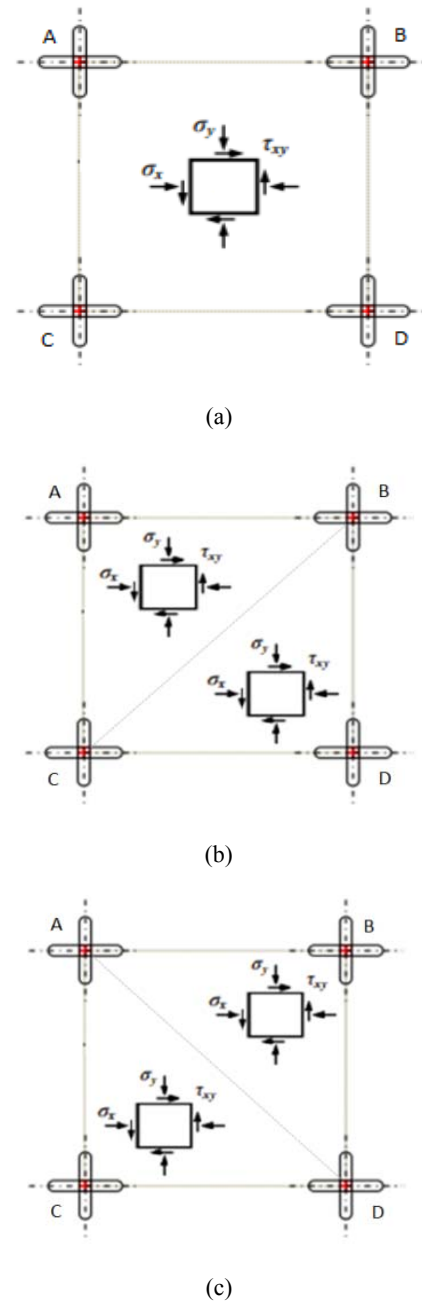

(b)

(c)

Fig. 1: (a) Distribution of linear indents and centroid subdivision from diagonals (b) CB and (c) AD. σ_x, σ_y, τ_{xy} are the stress components evaluated

shows the vertices (A, B, C and D) of the square. Each vertex is defined by the intersection of two linear micro-indents that form a cross. Through this distribution of 8 indents, it was possible to determine the residual stress components in the centroid of the square and also, in each centroid of four right triangles, which are shown in Fig. 1b and 1c. As mentioned above, each linear micro-indent was introduced using a unique design indenter. It is important to mention that from this type of indentation it was possible to reduce the measurement error.

For obtaining the stress components in the centroid of the square above through the coordinates of the vertices, it is necessary to implement a procedure that was developed in previous work (Díaz and Mammana, 2012). Regarding the stress components in the centroid of each triangle, the procedure establishes, first, to determine three components of residual deformation:

$$\varepsilon_x = \frac{l_x - l'_x}{l'_x} \tag{1}$$

$$\varepsilon_y = \frac{l_y - l'_y}{l'_y} \tag{2}$$

$$\varepsilon_h = \frac{l_h - l'_h}{l'_4} \tag{3}$$

In these expressions, l_x and l'_x correspond to the horizontal leg of the triangle and, l_y and l'_y correspond to the vertical leg, in both cases, before and after the thermal distension, respectively. Moreover, l_h and l'_h correspond to the hypotenuse, also before and after the distension. Then, the tangential component can be obtained:

$$\gamma_{xy} = 2 \cdot \varepsilon_h - \varepsilon_x - \varepsilon_y \tag{4}$$

Finally, the stress plane state evaluated for the case of a linear elastic, homogeneous and isotropic material can be expressed as (Gere, 2004):

$$\sigma_x = k_1 \cdot \varepsilon_x + k_2 \cdot \varepsilon_y \tag{5}$$

$$\sigma_y = k_1 \cdot \varepsilon_y + k_2 \cdot \varepsilon_x \tag{6}$$

$$\tau_{xy} = G \cdot \gamma_{xy} \tag{7}$$

where, $k_1 = E / (1 - v^2)$, $k_2 = v \cdot k_1$, E and G are the longitudinal and transverse elastic modulus, respectively and v is the Poisson's ratio.

It should be noted that three independent measurements of the vertex coordinates were performed before and after the distension treatment. Then, Eq. (5), (6) and (7) allowed obtaining nine values of the components σ_x, σ_y and τ_{xy} for each centroid evaluated. The values analysed in this study corresponded to the mean values of these components.

The error of this method is ±0.9 MPa (Díaz *et al.*, 2010). The process of coordinate measurement was carried out at 20±0.2°C, with a maximum variation of 0.01°C/min. It is indispensable to state that if the variation is higher than that value, the error will increase significantly.

Table 1: Stress components (MPa)

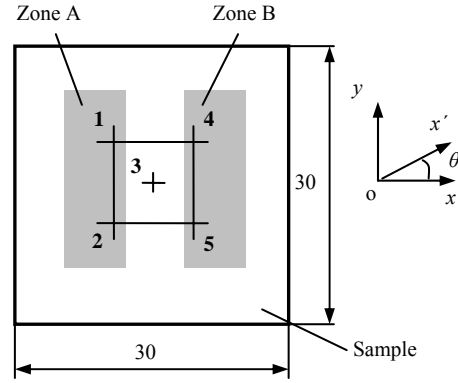| Points	σ_x	σ_y	τ_{xy}
1	-47.0	-37.6	-2.1
2	-42.4	-36.0	0.3
3	-43.1	-32.9	-3.8
4	-44.4	-29.8	-1.5
5	-39.9	-28.3	-2.6

Fig. 2: Centroids evaluated in the sample. The units are in mm

RESULTS AND DISCUSSION

Figure 2 shows the location of the five centroids evaluated in this study. The points 1, 2, 4 and 5 are the vertices of a square of 7 mm on the side. The centroid of this square is point 3. It should be noted that the direction x corresponds to the rolling direction.

The values of the stress components σ_x, σ_y and τ_{xy} are shown in Table 1. In this table, it can be observed a high difference between the values of normal and tangential components, approximately one order of magnitude. Moreover, the component σ_x is larger than σ_y, which was expected since the rolling direction corresponds to the x-axis. The average difference between σ_x and σ_y is around 25%. This difference is lower at the points 1 and 2 (zone A) and higher at the points 4 and 5 (zone B). Also, for both directions evaluated, the values of the components σ_x and σ_y at point 3 would be the mean values of the remaining four points. Regarding the component σ_y, the values at the points in zone A are similar. The same occurs with the values at the points corresponding to the zone B.

The measurement error, which is ±0.9 MPa, can be considered small for the components σ_x and σ_y (approximately 2%), but high for the tangential component τ_{xy} (around 40%). It is essential to indicate that the available techniques for residual stress determination, such as the hole drilling method and X-ray diffraction, introduce an error of approximately ±25 MPa. By using these techniques, the present work could not have been carried out.

It is noteworthy that the values of residual stress components will be modified when the evaluated direction changes. From σ_x, σ_y and τ_{xy}, it is possible to determine the normal and tangential components for any direction (Gere, 2004):

Table 2: Principal components (MPa)

Points	σ_p	σ_q
1	-47.0	-37.6
2	-43.3	-35.1
3	-43.8	-32.5
4	-44.6	-29.6
5	-41.0	-27.1

Table 3: Principal directions

Points	α (°)
1	1.5
2	-19.7
3	-10.6
4	-5.1
5	-16.7

$$\sigma_{x'} = \frac{\sigma_x + \sigma_y}{2} + \frac{\sigma_x - \sigma_y}{2}\cos 2\theta + \tau_{xy} \cdot \sin 2\theta \qquad (8)$$

$$\tau_{x'y'} = -\frac{\sigma_x - \sigma_y}{2}\sin 2\theta + \tau_{xy} \cdot \cos 2\theta \qquad (9)$$

In these equations, θ is the variable angle between the directions of x and x', as shown in Fig. 2. It is important to mention that the components $\sigma_{x'}$ and $\tau_{x'y'}$ vary continuously with the angle θ (Timoshenko and Goodier, 1970).

By using Eq. (8) and (9), the principal components of residual stress were obtained. Table 2 shows these components, which correspond to the compressive maximum (σ_p) and minimum (σ_q). It should be noted that the directions associated with σ_p and σ_q are called principal directions and also, they are perpendicular. For our case, the mean value of the differences between both components is also close to 25%. At points 1 and 2 (zone A), the difference is smaller than that value and, at points 3 and 4 (zone B), the difference is more significant. The component σ_q shows similar values at the points of the zone A and also, at the points of the zone B. When the values of Table 1 and 2 are evaluated, it is observed that the components σ_x and σ_p are similar and, furthermore, σ_y and σ_q are also similar. These similarities mean that the principal directions are very close to the reference axes, in all centroids evaluated. In particular, the direction associated with the compressive maximum (σ_p) is near the rolling direction (x-axis), which corroborates results obtained in previous works (Diaz *et al.*, 2012, 2015).

At each centroid evaluated, the values between those directions (angle α) are shown in Table 3. In this table, the values of angle α are within a range of 21°. The value at point 3 (central zone) would be an average of the rest. The values obtained for the angle α corroborate the analysis carried out from Table 1 and 2, where the components σ_x and σ_p show similar values and therefore, the associated directions would be close. Figure 3 shows the angular range in which the principal directions are found.

It is imperative to mention that the components $\sigma_{x'}$ and $\tau_{x'y'}$ can be represented, for all directions, using a
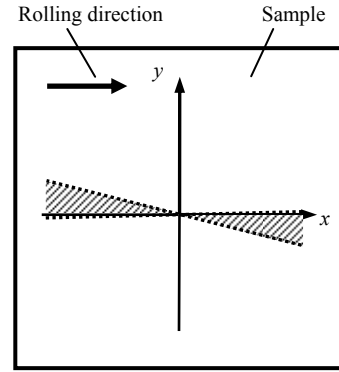

Fig. 3: Principal direction angular range

graph known as Mohr's circle (Timoshenko and Goodier, 1970). This graph helps to understand the link between normal and tangential components, for all planar directions. Moreover, from this circle, it is possible to observe the ranges in which those components fluctuate.

Figure 4 shows the Mohr's circles for each centroid evaluated. It is critical to mention that each point of each circle represents the normal ($\sigma_{x'}$) and tangential ($\tau_{x'y'}$) components associated with an arbitrary direction x', which is rotated by an angle θ regarding the x-axis (Fig. 2). Moreover, the circle associated with point 3 could be considered as an average of the remaining circles. This observation takes into account the compressive maximum and minimum (intersections between the circles and abscissa axis) and also, the maximum value of the tangential component (radius of the circle).

It is possible to observe clear similarities in the circles corresponding to the centroids 1 and 2 (zone A) and also, in those associated with the centroids 4 and 5 (zone B). These similarities imply that the residual stress states corresponding to each zone are similar. In Fig. 2 it is possible to see that the abscissas at the points 1 and 2 are the same and also, the abscissas at the points 4 and 5 are also the same. Therefore, the residual stress states would be showing a small variation or gradient as a function of the rolling direction (x-axis). The same variation was previously observed for the components σ_y and σ_q. It is feasible to assume that these components will vary according to a periodic function along the x-axis, staying close to a mean value. It can be hypothesised that the values of these components could respond to a sinusoidal function, similar to their angular variation (Timoshenko and Goodier, 1970). This behaviour would be extended to the residual stress state.

Figure 4 also shows that all circles are orderly grouped. Each circle intersects the abscissa axis at two points that correspond to the values of the components σ_p and σ_q. It is possible to observe that the component σ_q is equispaced; therefore, the following expression is valid:

Table 4: Subtraction of principal components

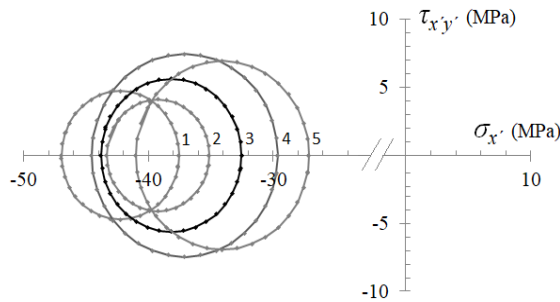| Points	$\Delta\sigma$ (MPa)
1	9.4
2	8.2
3	11.3
4	14.9
5	13.9

Fig. 4: Mohr's circles corresponding to the centroids 1, 2, 3, 4 and 5

$$\sigma_{q_{n-1}} - \sigma_{q_n} = k \tag{10}$$

In this expression, n is the number assigned to each centroid and k is a constant whose value is approximately 2.5 MPa. On the one hand, the circle corresponding to the centroid 1 (zone A) shows the maximum values (in absolute value) for σ_p and σ_q. On the other hand, the circle corresponding to the centroid 5 (zone B) shows the minimum values (in absolute value) for the same components σ_p and σ_q.

Furthermore, it is possible to express the subtraction between the principal components of residual stress as:

$$\Delta\sigma = \sigma_q - \sigma_p \tag{11}$$

This subtraction corresponds to the diameter of Mohr's circle. Table 4 shows the values obtained for $\Delta\sigma$. It is important to note that $\Delta\sigma$ is a precise measure of the anisotropy degree of the residual stress state, since each point of the Mohr's circle is associated with an x'-direction (Fig. 2). Ideally, a circle of infinite diameter corresponds to maximum anisotropy. In contrast, in a circle whose diameter is zero, the isotropy is perfect (the values of residual stress are the same for all directions). In the present case, on the one hand, the residual stress states that show the lowest anisotropy degree correspond to the centroids 1 and 2 (zone A). Moreover, the values are similar. On the other hand, at the centroids 4 and 5 (zone B), the anisotropy degree is higher and the values also are similar.

From the results shown in Fig. 4 and Table 4, it is possible to infer that the residual stress state and anisotropy degree in each centroid respond to the same behaviour pattern. Furthermore, when σ_x is analysed from Table 1, the values at centroids 1 and 2 are larger regarding those at centroids 4 and 5, respectively. Therefore, in the zone A, the local plastic deformation

will be higher in the rolling direction, although the difference regarding the zone B is small. In zone A, the values of σ_y are also higher. Therefore, in the direction perpendicular to the rolling direction, the local plastic deformation will also be higher in that zone. Furthermore, along with the direction y, the plastic deformation would not change because the values of σ_y are similar in each zone. The Mohr's circles corroborate this tendency since, in the centroids of the zone A, the normal components are more compressive for all directions and therefore, the local plastic deformation will be higher for all directions. Finally, the anisotropy levels at each zone and the anisotropy relationship between both zones would indicate a strict relationship in terms of local plastic deformation levels for all directions.

CONCLUSION

Different components of residual stress induced in a rolled sheet of AA 6082-T6 aluminium alloy were determined by using an optimised micro-indentation method. From a distribution of 8 micro-indents, the residual displacements were measured in 5 centroids of different geometric figures associated with that distribution. A high difference between values of normal and tangential components was found (approximately one order of magnitude). In the different zones evaluated in this study, the principal direction associated with the compressive maximum was found very close to the rolling direction (x-axis). The residual stress states and anisotropy degrees, evaluated from Mohr's circles, showed a small variation or gradient as a function of the rolling direction. Finally, from this small variation, it was possible to infer a strict relationship between both evaluated zones regarding the plastic deformation introduced in all planar directions.

ACKNOWLEDGMENT

CONFLICT OF INTEREST

The authors state that the current work does not present any conflict of interest.

REFERENCES

Coules, H.E., G.C.M. Horne, K. Abburi Venkata and T. Pirling, 2018. The effects of residual stress on elastic-plastic fracture propagation and stability. Mat. Design, 143: 131-140.

Dean, J., G. Aldrich-Smith and T.W. Clyne, 2011. Use of nanoindentation to measure residual stresses in surface layers. Acta Mater., 59(7): 2749-2761.

Díaz, F.V., R.E. Bolmaro, A.P.M. Guidobono and E.F. Girini, 2010. Determination of residual stresses in high speed milled aluminium alloys using a method of indent pairs. Exp. Mech., 50(2): 205-215.

Díaz, F.V. and C.A. Mammana, 2012. Study of Residual Stresses in Conventional and High-speed Milling. In: Filipovic, L.A. (Ed.), Milling: Operations, Applications and Industrial Effects. Nova Science Publishers, Inc., New York, pp: 127-155.

Díaz, F.V., C. Mammana and A. Guidobono, 2012. Evaluation of residual stresses induced by high speed milling using an indentation method. Modern Mech. Eng., 2(4): 143-150.

Díaz, F.V., C.A. Mammana and A.P.M. Guidobono, 2015. Evaluation of residual stresses in low, medium and high speed milling. Res. J. Appl. Sci. Eng. Technol., 11(3): 252-258.

Dotson, C.L., R. Harlow and R.L. Thompson, 2003. Fundamentals of Dimensional Metrology. 5th Edn., Thompson Delmar Learning, New York.

Gao, Y.K., M. Yao and J.K. Li, 2002. An analysis of residual stress fields caused by shot peening. Metall. Mater. Trans. A, 33: 1775-1778.

Gere, J.M., 2004. Mechanics of Materials. 5th Edn., Brooks/Cole, Pacific Grove, CA.

Lee, Y.H. and D. Kwon, 2003. Measurement of residual-stress effect by nanoindentation on elastically strained (1 0 0) W. Scripta Mater., 49(5): 459-465.

Lu, J., 1996. Handbook of Measurement of Residual Stresses. Fairmont Press Inc., Lilburn, GA.

Niku-Lari, A., 1983. Influence of residual stresses introduced by shot peening upon the fatigue life of materials. Exp. Tech., 7(3): 21-25.

Noyan, I.C. and J.B. Cohen, 1987. Residual Stress Measurement by Diffraction and Interpretation. Springer Verlag, Berlin.

Rendler, N.J. and I. Vigness, 1966. Hole-drilling strain-gage method of measuring residual stresses. Exp. Mech., 6(12): 577-586.

Rowlands, R.E., 1987. Residual Stresses. In: Kobayashi, A. (Ed.), Handbook on Experimental Mechanics. Prentice-Hall, New Jersey, pp: 768-813.

Schwach, D.W. and Y.B. Guo, 2006. A fundamental study on the impact of surface integrity by hard turning on rolling contact fatigue. Int. J. Fatigue, 28(12): 1838-1844.

Suresh, S. and A.E. Giannakopoulos, 1998. A new method for estimating residual stresses by instrumented sharp indentation. Acta Mater., 46(16): 5755-5767.

Timoshenko, S.P. and J.N. Goodier, 1970. Theory of Elasticity. 3rd Edn. McGraw-Hill, New York.

Toribio, J., 1998. Residual stress effects in stress-corrosion cracking. J. Mater. Eng. Perform., 7(2): 173-182.

Torres, M.A.S. and H.J.C. Voorwald, 2002. An evaluation of shot peening, residual stress and stress relaxation on the fatigue life of AISI 4340 steel. Int. J. Fatigue, 24(8): 877-886.

Wang, S., Y. Li, M. Yao and R. Wang, 1998. Compressive residual stress introduced by shot peening. J. Mater. Proc. Tech., 73(1-3): 64-73.

Withers, P.J., 2007. Residual stress and its role in failure. Rep. Prog. Phys., 70(12): 2211-2264.

Wyatt, J.E. and J.T. Berry, 2006. A new technique for the determination of superficial residual stresses associated with machining and other manufacturing processes. J. Mater. Proc. Tech., 171(1): 132-140.

Wyatt, J.E. and J. Berry, 2009. Mapping of superficial residual stresses in machined components. J. Ind. Technol., 25(1): 1-8.